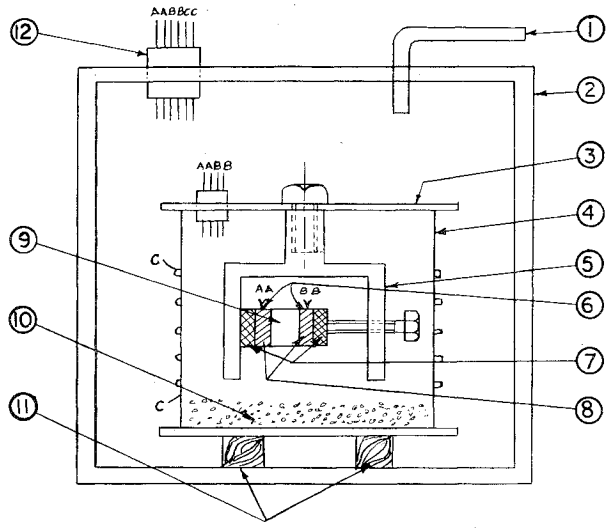

Fig. 1 Apparatus for conductivity measurement: 1) connection to vacuum pump; 2) vacuum chamber; 3) Asbestos sheet; 4) electric heater; 5) clamping device; 6) thermocouple wires; 7) Teflon sheet; 8) copper discs; 9) smaple; 10) glass wool; 11) wooden block; 12) pipe filled with epoxy resin; AA) terminals of the first thermocouple wires; BB) terminals of the second thermocouple wires; CC) terminals of the wire heater.

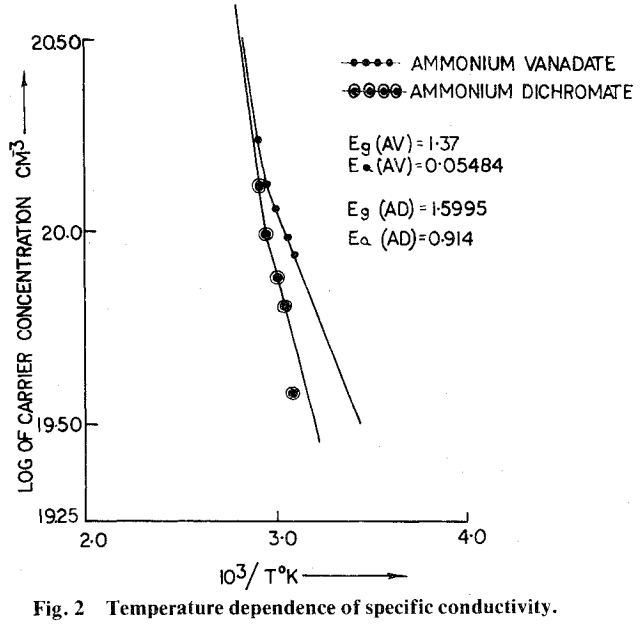

Fig. 2 Temperature dependence of specific conductivity.

can provide chain carriers by exciton formation easier than ammonium dichromate, because the energy required for the exciton formation in case of ammonium vanadate is much less than that required for ammonium dichromate. Since the rate of reaction is proportional to the number of collisions taking place per second, the rate of collision would be high if the concentration of the reactants are high and their mean free path is small. The relation (4) developed by Aigrain and Dugas[5,6] for charge carrier concentration and the number of species adsorbed on the surface of semiconductor catalyst indicates that the higher the charge carrier concentration, the higher the concentration of the adsorbed species.

$$N_f = \left[\frac{k}{2\pi e} n_0 V_f \right]^{1/2} \tag{4}$$

Figure 3 shows that the charge carrier concentration in case of ammonium vanadate is higher at all temperatures than in case of ammonium dichromate. Further the values of mean free path of the charge carriers, calculated from Eq. (5), indicate that at each temperature the mean free path in case of

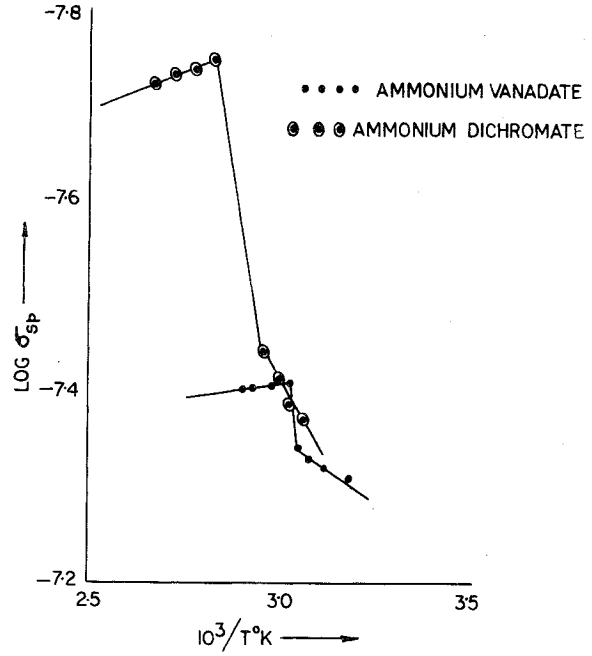

Fig. 3 Variation of charge carrier concentration with temperature.

ammonium vanadate is shorter than in case of ammonium dichromate (Table 1).

$$l = \left[\frac{2KmT}{n_0 e^2} \right]^{1/2} \tag{5}$$

These observations suggest that the higher the concentration and mobility[6] of the charge carrier of the catalyst, the higher the catalytic activity to expedite surface reaction rates. These conclusions help to explain the higher activity of ammonium vanadate over ammonium dichromate in reducing the ignition delay of the present hybrid propellant system.

References

[1] Munjal, N.L., "Ignition Catalysts for Furfuryl Alcohol-Red Fuming Nitric Acid Bipropellants," *AIAA Journal*, Vol. 8, May 1970, pp. 980-981.

[2] Munjal, N.L., Prasad, J., and Ghosh, S.C., "Ignition of Non-Hypergolic Rocket Fuels with Fuming Nitric Acid under Suitable Conditions," *AIAA Journal*, Vol. 10, Oct. 1972, pp. 1345-1346.

[3] Munjal, N.L. and Parvatiyar, M.G., "Ignition of Hybrid Rocket Fuels with Fuming Nitric Acid as Oxidant," *Journal of Spacecraft and Rockets*, Vol. 11, June 1974, pp. 428-430.

[4] Adler, D., Brooks, H., "Theory of Semiconductor-To-Metal Transition," *Physics Review*, Vol. 155, March 1967, pp. 826-840.

[5] Stone, F.S., *Chemistry of the Solid State* Butterworth, London, 1955, p. 367.

[6] Clark, A., *The Theory of Adsorption and Catalysis*, Academic Press, New York, 1970, pp. 196-197, 343.

Improved Determination of Apogee Motor Pointing

R.G. Lagowski* and R.J. Ferguson*
Telesat Canada, Ottawa, Canada

Introduction

THE first two geosynchronous communications satellites of Telesat Canada (ANIK I, ANIK II)[1] experienced

Received June 19, 1975; revision received September 11, 1975.
Index Categories: Spacecraft Attitude Dynamics and Control; Spacecraft Navigation, Guidance, and Flight-Path Control Systems.

*Programmer Analyst, Satellite Control Division.

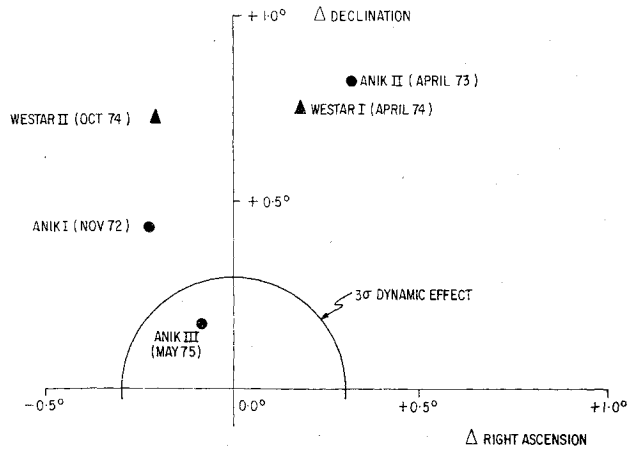

Fig. 1 AMF pointing errors for the ANIK and WESTAR satellites (Δ = thrust vector—mission attitude solution).

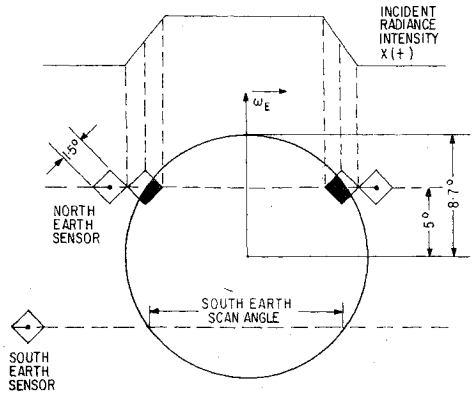

Fig. 2 Idealized geometry for sensor scan of the Earth at geosynchronous orbit normal attitude and the radiance $x(t)$ incident on the Earth sensor.

anomalously large apogee motor firing (AMF) tip-off (approximately 1°, see Fig. 1), which necessitated corrective maneuvers. Tip-off is defined here as the difference between the pre-AMF attitude determined from the attitude sensor data, and the AMF thrust vector determined by an orbit-matching procedure. Random engine and satellite dynamic effects, estimated to be on the order of 0.3°, could not account for the much larger systematic discrepancies in declination, although differences in right ascension were small and random. When it was discovered that the WESTAR (Fig. 1) and INTELSAT IV missions exhibited a similar anomaly, though with varying magnitudes, the authors investigated possible deficiencies in the attitude determination algorithm common to all three satellites (ANIK, WESTAR, INTELSAT IV). This led to the development of a model of the Earth's atmosphere as seen by the sensors, and a model of the effects of the sensing system on the Earth sensor input waveform.† These models were used during the recent ANIK III mission, and the improved attitude solutions determined prior to AMF eliminated a large portion of the unexplained tip-off effect.

Attitude Determination System

The spin axis declination is particularly sensitive to the Earth reference direction defined by a pair of redundant, radially-mounted sensors separated by 10° in elevation and 45° in azimuth. These detectors contain germanium filters which pass infrared radiation (14.25-15.75μ) to thermistor bolometers with 1.5° × 1.5° diamond-shaped fields of view (FOV), as shown in Fig. 2. The bolometer output pulse is approximately rectangular, with amplitude equivalent to the Earth radiance seen by the sensor, and width equal to the time taken by the FOV to scan between Earth horizons. These pulses are combined, amplified and telemetered to the ground station, together with two sun pulses, and converted by an attitude pulse digitizer (APD) to digitized time references for the leading and trailing edges of the pulses.

†Brewer and Soubirou have independently developed similar models for ESRO IV.[2]

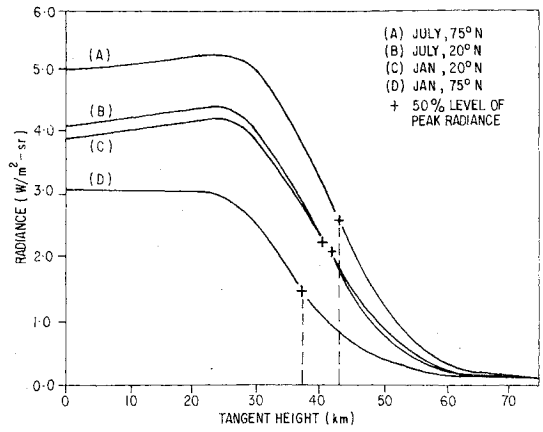

Fig. 3 Radiance profiles for the 14.25-15.75 μ CO_2 spectral band.

The attitude determination computer program contains a batch filter which estimates, from the telemetered sensor data, the spin axis attitude and constant sensor alignment biases. The technique of weighted least squares, with a priori statistics, is used to reduce the effects of random observation noise. From the satellite orbital position and an attitude estimate, the corresponding sensor observations are computed, and the residuals (differences between the predicted values and the observed sensor output) are used to recursively correct the initial estimate. In previous missions, the Earth data residuals showed a variable bias in the Earth scan angle as a function of time. This effect has been a problem with respect to accurate attitude determination, and has now been minimized through the use of the two models described in the following sections.

Model of the Earth Sensing System

The Earth sensor is oriented such that its FOV is filled in an approximately linear manner when the satellite is in operational configuration (geosynchronous orbit, polar attitude). As a result, the radiance incident on the bolometer during a spin frequency scan of the Earth can be represented by the trapezoidal ramp $x(t)$ indicated in Fig. 2.[3] The output of each bolometer is given by the convolution integral

$$y(t) = x(t) \otimes h(t) = \int_0^t x(\tau) h(t-\tau) \mathrm{d}\tau \qquad (1)$$

where $h(t) = (1/c)\ \exp(-t/c)$ is the bolometer impulse response function, with time constant $c \simeq 3$ msec. Capacitative coupling of $y(t)$ to an on-board amplifier yields

$$z(t) = y(t) - 1/T \int_0^t z(\tau) \mathrm{d}\tau \qquad (2)$$

where the time constant T of the coupling network is about 300 msec. The signal $z(t)$ is transmitted to a ground station where it is electronically differentiated, and the leading- and trailing-edge derivative pulses are threshold detected at a fixed ratio relative to the peak (usually 60%).

During a transfer orbit, $x(t)$ does not always have the trapezoidal form shown in Fig. 2. In order to model how this affects the observation times, a program was developed to calculate horizon crossing times for the center of the sensor

Table 1 Thrust vectors and attitude solutions[a] for the ANIK missions

		Thrust vector	Attitude solution type: Mission result	Uncorrected algorithm	Corrected algorithm
ANIK I:	RA	336.4	336.6	336.7	336.5
	DEC	-22.8	-23.2	-23.0	-22.8
ANIK II:	RA	114.2	113.9	113.7	113.8
	DEC	-23.1	-23.9	-24.3	-23.1
ANIK III:	RA	127.8	127.9	127.6	127.9
	DEC	-22.5	-22.7	-23.7	-22.7

[a] Attitude solution accuracy is 0.25° (3σ) in right ascension (RA) and declination (DEC).

FOV. Also, intensity input to the Earth sensor was simulated as a function of the angle χ between the spin axis and satellite-Earth vector, distance r to the Earth, and spin speed ω. If the FOV is divided into N^2 partitions, the radiance intensity is $x(t) = (m/N^2)E$, where m is the number of partitions filled at time t, and E is the peak radiance seen by the sensor. The resultant digital waveforms were then modified by numerical integration of Eqs. (1) and (2) to account for the deformation due to the electronics. Finally, the pulses were processed by a simulated APD to determine the threshold level crossing times. A table containing the differences (delays) between these times and the calculated horizon crossing times was generated for the various values of χ, r, ω, and APD setting, and was then incorporated into the attitude determination program, together with an interpolation routine (linear in ω, quadratic in r and χ).

In addition to improving the attitude solution accuracy, use of this table also reduced the large observation residuals that occurred as the Earth scan angles decreased. However, for scan angles smaller than 7°, less than half of the FOV was filled during the scan, and since this situation was not modeled, all Earth sensor data less than 7° were culled during the ANIK III mission.

Radiance Profile of the Earth

For the first two ANIK missions, the attitude determination algorithm defined the Earth as a solid sphere with radius 1 ERU (6378.160 km), whereas the Earth sensors are sensitive to the infrared radiation emitted by CO_2 in the atmosphere. The thermal radiance discontinuity between Earth and space at opposite horizons, which is used to define the Earth reference direction, is actually a gradient—the horizon radiance profile. The CO_2 band has traditionally been chosen because of its relatively constant atmospheric mixing ratio, which minimizes the profile sensitivity to atmospheric variations, and because it is a strong absorption band, which causes the radiation to originate mainly from relatively high atmospheric levels where large temperature variations and clouds are avoided. To minimize the effects of reflected solar radiation, the 14.25-15.75μ region of the CO_2 spectral band is being used. Figure 3 contains radiance profiles as a function of tangent height, representing maximum seasonal and latitude variations for this spectral region.[4] Tangent height is the distance along the geocentric radius vector, from the Earth's surface to the point where the radius vector is normal to the sensor line of sight. The effective increase in the Earth's radius seen by the sensor varies between 38 and 44 km, at a threshold of 50% of peak radiance. Therefore, the Earth's radius was redefined to be 6418.160 km in the attitude determination program, which led to a reduction of the observation residuals and removal of the remaining attitude discrepancy.

Results

Sensor data prior to AMF for the ANIK I and ANIK II missions were analyzed with and without the model corrections to the attitude determination algorithm, and compared to the mission results and the thrust vectors calculated from the orbit-matching analysis. The solutions from both algorithms were compared in the ANIK III mission. The results (Table 1) indicate that the corrected declination (column 4) was within 0.2° of the reference thrust vector (column 1) for all missions, whereas the uncorrected algorithm (column 3) gave discrepancies of as much as 1.2°. Since AMF attitude error is a sensitive parameter, with regard to reaction control system fuel consumption (requiring as much as two-thirds of a year stationkeeping fuel per degree of error), ANIK III was a most successful mission.

In conclusion, the attitude determination model modifications described in this Note represent a solution of the previously unresolved tip-off error for the ANIK missions, and may be extended to similar systems experiencing the same problem.

References

[1] Kowalik, H., "Telesat Satellite Control System," *AIAA Progress in Astronautics and Aeronautics: 5th Communications Satellites – Technology,* to be published.

[2] Brewer, M.J. and Soubirou, J., "Evaluation of the ESRO IV Satellite Horizon Crossing Indicator Performance," *Journal of Spacecraft and Rockets,* Vol. 12, April 1975, pp. 235-241.

[3] Wright, W.H., Grise, A.J., and Ferguson, R., "Earth Sensor Processing—A Preliminary Study," TR-01-74-01, Jan. 1974, Telesat Canada, Ottawa, Canada.

[4] Bates, J.C., Hanson, D.S., House, F.B., Carpenter, R.O'B., and Gille, J.C., "The Synthesis of 15μ Infrared Horizon Radiance Profiles From Meteorological Data Inputs," NASA, CR-724, April 1967.

Solar Absorptance of Second Surface Mirrors for High Angles of Incidence

James W. Stultz*
Jet Propulsion Laboratory, Pasadena, Calif.

Introduction

MEASUREMENTS have indicated an increase rather than a decrease in the solar absorptivity of second surface mirrors at angles of incidence greater than 80°. Unpublished test data by the Aerojet Electrosystem Company, Azusa, Calif (contact C. B. Fisher) was the first to suggest that such a phenomenon was occurring. Measurements in the Jet Propulsion Laboratory's Celestarium supported Aerojet's results. The JPL measurements were made on a second surface mirrored radiator like those currently being monitored on the Nimbus E Microwave Spectrometer experiment. These measurements were made just prior to the launch of Nimbus E and indicated that the radiator temperature would be warmer than expected, which has proved to be the case. Helios, a

Presented as Paper 74-670 at the AIAA/ASME 1974 Thermophysics and Heat Transfer Conference, Boston, Massachusetts, July 15-17, 1974; submitted April 23, 1975; revision received October 28, 1975. This paper presents the work of one phase of research carried out at the Jet Propulsion Laboratory, California Institute of Technology, under NASA Contract NAS 7-100.

Index category: Thermal Surface Properties.

*Member of the Technical Staff, Thermophysics and Fluid Dynamics Section, Applied Mechanics Division. Member AIAA.